Pharmaceutical Sciences Asia

Pharm Sci Asia 2026; 53(3), 294-308

DOI:10.29090/psa.2026.03.25.9140

Research Article

Pharmacokinetic modeling and simulation of isoniazid dosing for different N-acetyltransferase 2 phenotypes in Thai tuberculosis patients

Thanakorn Surarak[1,5], Pramote Tragulpiankit[1*], Surakameth Mahasirimongkol[2], Hutcha Sriplung[3], Usanee Ungcharoen[4], Wichit Nosoongnoen[1*]

[1] Department of Pharmacy, Faculty of Pharmacy, Mahidol University, Bangkok, Thailand
[2] Information and Communication Technology Center, Ministry of Public Health, Nonthaburi, Thailand
[3] Epidemiology Unit, Faculty of Medicine, Prince of Songkla University, Songkhla, Thailand
[4] Division of Tuberculosis, Department of Disease control, Ministry of Public Health, Bangkok, Thailand
[5] Division of Pharmacology, Department of Preclinical Science, Faculty of Medicine, Thammasat University, Pathumthani, Thailand

ABSTRACT

The metabolism of isoniazid (INH) is influenced by N-acetyltransferase 2 (NAT2) genetic polymorphisms, which regulate its acetylation rate. This study aimed to optimize INH dosages for Thai patients with tuberculosis (TB) based on their NAT2 phenotypes. INH plasma concentrations were measured using HPLC-MS/MS. Pharmacokinetic (PK) parameters, including the absorption constant (k_a), apparent volume of distribution (V_d/F), and elimination constant (k_e) were estimated via population PK modeling with Phoenix® NLME software. A one-compartment model with first-order absorption and elimination was employed using the FOCE ELS algorithm. Covariate analysis indicated that the PK of INH was substantially influenced by the NAT2 phenotype and body weight. Model selection was guided by -2LL, AIC, and BIC statistics, while model validation was evaluated via goodness-of-fit plots, bootstrap analysis, and visual predictive checks. Subsequently, Monte Carlo simulations in Oracle® Crystal Ball software were used to predict plasma INH concentrations for each NAT2 phenotype. The study suggested optimal daily INH dosages to achieve therapeutic plasma levels of 3–6 µg/mL: 225-250 mg for slow acetylators (SA), 275-300 mg for intermediate acetylators (IA), and 400-450 mg for rapid acetylators (RA). These dosage adjustments aim to improve treatment efficacy and reduce drug toxicity risks. By tailoring dosages to the NAT2 phenotype, this pharmacogenetic approach enhances the safety and effectiveness of TB therapy, offering a valuable framework for personalized medicine, particularly in genetically diverse populations like Thai patients.

Keywords:
Isoniazid; NAT2 phenotype; Pharmacokinetic-pharmacodynamic simulation; Modeling

1. INTRODUCTION

Tuberculosis (TB) remains a global health crisis, with *Mycobacterium tuberculosis* (MTB) as the causative agent [1]. For TB treatment, both the WHO 2022 and Thai 2021 Guidelines recommend standard first-line regimens, typically comprising two months of isoniazid (INH), rifampicin, pyrazinamide, and ethambutol, followed by four months of INH and rifampicin [2, 3]. Isoniazid serves as a key component in treatment regimens for newly diagnosed TB patients. It is metabolized primarily through N-acetyltransferase 2 (NAT2)-mediated acetylation in the liver and intestine [4]. Based on NAT2 enzyme activity, individuals are classified as slow (SA),

***Corresponding author:**
* Wichit Nosoongnoen Email: wichit.nos@mahidol.ac.th
* Pramote Tragulpiankit Email: pramote.tra@mahidol.ac.th

intermediate (IA), or rapid (RA) acetylators [5]. In the Thai population, the distribution of acetylator phenotypes ranged as follows: 22-52% for SA, 36-62% for IA, and 10-15% for RA [6-9]. In contrast, the distribution of acetylator phenotypes in Korean and Japanese populations differs from that observed in the Thai population. The proportion of RA is higher among Koreans (39–41%) [10, 11] and Japanese (36–53%) [12-15] than among Thais. Conversely, the proportion of SA is lower in Koreans (11–15%) and Japanese (9–10%) compared with Thais. SA are at higher risk of INH hepatoxicity, even with standard doses, whereas RAs may experience treatment failure due to subtherapeutic INH level [14, 15]. Tailoring INH dosage regimens to match the *NAT2* genotype could mitigate the risk of INH toxicity, particularly hepatoxicity, and enhance clinical efficacy [15]. To enhance TB treatment, in Thailand, tailoring INH dosages to specific NAT2 phenotypes in TB treatment remains limited. By integrating population pharmacokinetic (PopPK) simulation techniques, dosage regimens can be optimized for specific patient groups. This study aimed to address this gap by characterizing the PK parameters of INH and simulating appropriate dosage regimens for Thai TB patients based on their NAT2 phenotypes.

2. MATERIALS AND METHODS

2.1. Patients, study treatment, and sample collection

The study was conducted under the IRB ethical approval (COE.NO.MU-DT-PY-IRB 2023/043.0410). TB Patients in study entitled "Assessment of pharmacokinetic parameters and development of isoniazid dosing formula based on N-acetyltransferase 2 genotype in Thai tuberculosis patients" were included [8]. Thirty-nine patients were recruited from three hospitals in Southern Thailand. These patients received standard TB treatment, which obtained INH (4-6 mg/kg), rifampicin (8-10 mg/kg), ethambutol (15-20 mg/kg), and pyrazinamide (20-30 mg/kg). A whole blood sample was collected for liver function tests and NAT2 genotyping at the screening phase. Blood samplings were performed at 0 (pre-treatment), 1, 2, 4, and 6 hours after INH administration [8].

The inclusion criteria were as follows: 1) Newly pulmonary TB patient; 2) Age between 18 and 65 years old; 3) Receiving INH daily. The exclusion criteria included: 1) patients with abnormal values for liver function testing before anti-TB drugs treatment; 2) patients with underlying hepatic diseases, including cirrhosis, chronic hepatitis, and acute viral hepatitis B or C; 3) patients with HIV-positive; 4) patients with extremely illness (survival rate less than 9 months); 5) patients with hepatotoxic drugs: methotrexate, phenytoin, carbamazepine, warfarin, theophylline, phenobarbitone, valproate, atenolol, labetalol, salicylates, allopurinol, quinine, quinidine, fluconazole, cimetidine, ethionamide, verapamil, probenecid, TCA, and halothane; 6) patients with pregnancy or lactation; 7) patients with prolonged use of steroid; 8) patients who were a current alcohol drinker (within 1 month). The demographic and physiological data of patients were extracted from the medical records including age, gender, body weight, height, alanine aminotransferase (ALT), aspartate aminotransferase (AST), alkaline phosphatase (ALP).

2.2. NAT2 genotyping

A haplotype-specific polymerase chain reaction (PCR)-based method (HS-PCR) was performed to determine *NAT2* genotyping [8, 16]. DNA from the whole blood sample was extracted using a commercial kit (QIAamp DNA blood mini kit, QIAGEN GmbH, Hilden, Germany), and then spectrophotometry was used to quantify DNA content. Six specific primer pairs (forward and reverse) were used for each of the most common haplotypes found in Thai populations, including NAT2*4, *5B, *6A, *7B, *12A, and *13A. Each of the haplotypes was divided into 2 groups including high-activity enzymatic haplotypes (NAT2*4, *12A, and *13A), and low-activity enzymatic haplotypes (NAT2*5B, *6A, and *7B). PCR amplification was conducted by Bio-RaD T100 Thermocycler (Hercules, CA, USA) as described in previous study [16]. The RA phenotype was either homozygous or heterozygous genotypes of high-activity enzymatic haplotypes. The SA phenotype was interpreted by a combination of low-activity enzymatic haplotypes as either homozygous or heterozygous genotypes. The IA phenotype was determined by heterozygous haplotypes of high and slow enzymatic activity [6-8, 16].

2.3. Determination of INH plasma levels

After anti-TB initiation for fourteen days, blood sampling from patients in the study at time 0, 1, 2, 4, and 6 hours of drug administration. The separated plasmas were immediately stored at -80°C until performing a bioanalysis. The plasma sample preparation was conducted with the protein precipitation method. INH plasma concentration was measured by high-performance liquid chromatography-tandem mass spectrometry (HPLC-MS/MS) using an an ACQUITY UPLC H-Class system (Waters, Watford, UK) with a Kinetex XB-C18 column (2.1×100 mm, Phenomenex, Torrance, CA, USA) by positive ion mode in MS with transitions of m/z 138.20 to 121.10 for INH and of m/z 237.03 to 194.03 for carbamazepine as internal standard. The linear range of INH was between 2 and 50 ng/mL [8].

2.4. Population pharmacokinetic and model analysis

A PopPK analysis was performed by using the software Phoenix® NLME (version 8.5.2.4 Certara USA, Inc., Princeton, NJ). The Phoenix® software has been granted the license to the Faculty of Pharmacy, Mahidol University. Four algorithms including QRPEM, FOCE ELS, FOCE E_B, and IT2S-EM were applied to the modeling procedure. The comparisons of models were evaluated using -2LL (twice the negative Log-Likelihood) or OFV (objective function value), AIC (Akaike Information Criterion), and BIC (Bayesian Information Criterion).

2.4.1. Base model

The PopPK modeling was conducted by the Maximum likelihood estimation (MLE) method to estimate the PK parameters such as rate of absorption (k_a), apparent clearance (CL/F) and apparent volume of distribution (V_d/F). The concentration profiles of INH were fitted with one and two compartment models based on first order absorbtion and elimination. Proportional, additive, log-additive, mixed, and power error models were investigated as models to account for residual variability. The inter-individual variability (IIV) in PK parameters of INH was estimated using an exponential error model. The exponential error model had the following formula: $P_i = P_{tv} \exp(\eta_i)$, where P_i meant the estimated PK parameter for individual *i*, P_{tv} meant the population typical value of that parameter, η_i meant the random variable for the individual *i*, normally distributed with mean 0 and variance ω^2. The final selection of the structural base model was performed by comparing differences of statistical significance (-2LL, AIC, and BIC) between the models.

2.4.2. Covariate model

After development of the base model, the potential covariates, including physiological (age, gender, body weight, height), genetic polymorphism (*NAT2* polymorphism) data and biochemical parameters (AST, ALT, ALP) were tested using stepwise forward selection followed by backward elimination steps. Covariates with a decrease in OFV values more than 3.84 ($p < 0.05$, with Chi-squared distribution, df = 1) were included in the base model according to the forward addition step. Then the covariates were removed from the full model one by one. Covariates with an increase in OFV values greater than 6.63 ($p < 0.01$, with Chi-squared distribution, df = 1) were retained in the final model. In the screening process, power models were applied for continuous covariates including age, body weight, and liver function. While exponential model were used for categorical covariate such as sex and NAT2 phenotypes.

2.4.3. Model validation

The model validation was evaluated by the goodness-of-fit (GOF) plots, nonparametic bootsrap method, and visual predictive check (VPC). To assess the accuracy of the PopPK model, GOF was identified using several diagnostic scatterplots, and the relationships between the scatterplots were as follows: observed (DV) vs population predicted (PRED) concentrations, DV vs individual predicted (IPRED) concentrations, conditional weighted residuals (CWRES) versus PRED, and CWRES versus time (IVAR). To assess model stability, the 2.5th, 50th, and 97.5th percentile of the bootstrap estimates were computed and compared to the final model parameter estimates. A nonparametic bootstrap method was conducted using 1,000 randomly resampled datasets generated from the original data. The VPC method was performed by simulating 1,000 virtual subjects based on the final model estimates. The observed data were graphically superimposed on the median, 95th, and 5th percentiles of the simulated concentration-time profile. To evaluate the predictive performance of the final model, the observed data were roughly distributed within the 95th and 5th predictive interval.

2.5. Model-based simulation of INH dosage

The population PK parameters including k_a (h^{-1}), V_d/F (L), CL/F (L/h) and k_e (h^{-1}) of the best potential population modeling calculated from Phoenix NLME® software were employed to predict the plasma C−T profiles using the Oracle® Crystal Ball performing with the one-compartmental approach. The Monte Carlo simulation of the software was conducted to generate 10,000 virtual patients at steady state conditions to establish the maximum plasma concentration (C_{max}), the area under the curve from 0 to 24 hours ($AUC_{0–24}$), and the area under the curve from 0 to infinity hour ($AUC_{0–\infty}$). The various dosage regimens (dose and dosing interval) of INH were employed to predict the C_{max}, $AUC_{0–24}$, and $AUC_{0–\infty}$. In addition, the percentage of patients having C_{max} of 3−6 µg/mL (PP3−6), C_{max} >6 µg/mL (PP6), and $AUC_{0–\infty} \geq 10.52$ µg.h/mL (PPA10), the percentage of probability target attainment (%PTA) of $AUC_{0–24}$/MIC >61.6 (%PTA50) were evaluated to select the optimal INH dosage regimens in each group of NAT2 acetylator. The MIC of 0.0312 µg/mL was used to calculate the %PTA50 to express 50% kill *M. tuberculosis* (EC50) [17]. The target attainment analysis using EC_{50} ($AUC_{0–24}$/MIC >61.6) and the PK/PD breakpoint of the %PTA >90% was defined as achieved goals [11].

Table 1. Demographic and clinical data of the study population.

Data	Number (%)	Mean ± SD	Median (range)
Number of patients	39 (100.00)	-	-
Gender, n (%) Male Female	 25 (64.10) 14 (35.90)	-	-
Age (years)	-	43.49 ± 13.59	46.00 (20.00-65.00)
Weight (kg)	-	53.09 ± 7.62	53.30 (39.20-72.90)
BMI (kg/m^2)	-	19.68 ± 3.11	19.38 (14.53-28.12)
INH Dose (mg)	-	296.15 ± 13.50	300.00 (250.00-300.00)
Laboratory parameter			
ALT (U/L)	-	16.92 ± 8.92	14.00 (5.00-40.00)
AST (U/L)	-	20.64 ± 7.67	19.00 (8.00-45.00)
ALP (U/L)	-	94.38 ± 31.78	91.00 (42.00-213.00)
Treatment outcomes, n (%)			
Cured	SA = 15 (38.46), IA = 14 (35.90), RA = 2 (5.13)		
Lost to follow-up	SA = 3 (7.70), IA = 0 (0.00), RA = 1 (2.56)		
Transferred out	SA = 1 (2.56)		
Changed diagnosis	-		
Died	SA = 0 (0.00), IA = 1 (2.56), RA = 2 (5.13)		

Abbreviations: ALP: alkaline phosphatase; ALT: alanine aminotransferase; AST: aspartate aminotransferase; BMI: body mass index; IA: intermediate acetylator; INH: isoniazid; kg: kilogram; L: liter; m^2: square meter; mg: milligram; n: number; NAT2: N-acetyltransferase 2; RA: rapid acetylator; SA: slow acetylator.

3. RESULTS

3.1. The demographic data of patients

A total 39 patients composed of 25 males and 14 females were recruited into this study. All blood samples were fully collected at 0, 1, 2, 4, and 6 hous, yielding a total of 195 samples (5 x 39) for population PK analysis. The mean ± SD of age, weight, BMI and INH dose were 43.49 ± 13.59 years, 53.09 ± 7.62 kg, 19.68 ± 3.11 kg/m^2 and 296.15 ± 13.50 mg, respectively. The demographic and clinical characteristics of participants are summarized in Table 1. The patient characteristics categorized by NAT2 phenotype of SA, IA, and RA are also presented in Table 2.

Table 2. Demographic data and predicted pharmacokinetic parameters categorized by NAT2 phenotype.

Parameter	NAT2 phenotype			
	All	SA	IA	RA
Number of patients, n (%)	39 (100.00)	19 (48.72)	15 (38.46)	5 (12.82)
Gender, n (%) Male Female	 25 (64.10) 14 (35.90)	 13 (68.42) 6 (31.58)	 9 (60.00) 6 (40.00)	 3 (60.00) 2 (40.00)
Age (years)	43.49 ± 13.59	43.26 ± 12.82	39.67 ± 14.26	55.80 ± 7.73
Weight (kg)	53.09 ± 7.62	54.74 ± 8.33	51.05 ± 7.58	52.98 ± 3.08
BMI (kg/m^2)	19.68 ± 3.11	19.68 ± 3.32	19.24 ± 3.01	20.97 ± 2.81
INH Dose (mg)	296.15 ± 13.50	297.37 ± 11.47	293.33 ± 17.59	300.00 ± 0.00
PK parameter				
k_a (h^{-1})	1.59 ± 0.05	1.58 ± 0.03	1.60 ± 0.06	1.57 ± 0.07
k_e (h^{-1})	2.78 ± 1.39	1.76 ± 0.003	2.96 ± 0.01	6.10 ± 0.01
V_d/F (L)	17.59 ± 4.29	18.54 ± 4.73	16.46 ± 4.04	17.34 ± 1.55
CL/F (L/h)	48.21 ± 25.34	32.65 ± 8.27	48.72 ± 11.88	105.82 ± 9.29

Values were expressed as mean ± SD. Abbreviations: BMI: body mass index; CL/F: apparent clearance; IA: intermediate acetylator; INH: isoniazid; k_a: absorption rate constant; k_e: elimination constant; kg: kilogram; L: liter; m^2: square meter; mg: milligram; n: number; NAT2: N-acetyltransferase 2; RA: rapid acetylator; SA: slow acetylator; V_d/F: apparent volume of distribution.

Table 3. Pharmacokinetic parameter estimates from the final model and bootstrap results.

Parameter	Final model		Bootstrap (n=1000)		Bias (%)
	Estimate	CV (%)	median	95% CI	
Fixed-effect					
k_a (h^{-1})	1.586	6.055	1.592	1.335–24.607	0.378
V_d/F (L)	17.384	6.708	17.074	12.259–24.605	-1.783
CL/F (L/h)	106.034	8.604	104.055	45.717–138.882	-1.866
dCl/FdNAT2$_{IA}$	-0.723	-13.753	-0.714	-1.024– -0.337	-1.245
dCl/FdNAT2$_{SA}$	-1.242	-7.488	-1.234	-1.537– -0.696	-0.644
dV_d/Fdwt	1.700	6.775	1.662	-0.222–3.653	-2.235
dCl/Fdwt	1.689	7.439	1.654	0.742–2.504	-2.072
Random-effect					
k_a (h^{-1})	0.016308	0.284	0.015844	0.010980–0.020704	-2.870
V_d/F (L)	0.000166	3.065	0.000207	-0.001747–0.002160	24.699
CL/F (L/h)	-0.000081	-2.706	-0.000083	-0.000171–0.000050	2.469
Residual viability					
Log-additive error	0.675	6.798	0.666	0.561–0.764	1.333

Abbreviations: CL/F: apparent clearance; dCl/FdNAT2$_{IA}$: effect intermediate acetylator (IA) on CL/F; dCl/FdNAT2$_{SA}$: effect slow acetylator (SA) on CL/F; dCl/Fdwt: effect body weight on CL/F; dV_d/Fdwt: effect body weight on V_d/F; h: hour; k_a: absorption rate constant; L: Litre; V_d/F: apparent volume of distribution; wt: body weight

Cl/F $_{RA}$ (L/h) = 106.034*(wt/53.09)^1.689*exp(-0.000081)

Cl/F $_{IA}$ (L/h) = 106.034*(wt/53.09)^1.689*exp(-0.723)* exp(-0.000081)

Cl/F $_{SA}$ (L/h) = 106.034*(wt/53.09)^1.689*exp(-1.242)* exp(-0.000081)

V_d/F (L) = 17.384*(wt/53.09)^1.7*exp(0.000166)

3.2. PopPK model development

The concentration−time (C−T) profile of INH was well fitted to a one-compartment model with first-order absorption and elimination using the first-order conditional estimation-extended least squares (FOCE ELS) algorithm. For the inter-individual variability or random effect could be expressed using an exponential model, while residual viability could be indicated by log-additive error model. For basic model, the OFV, AIC, and BIC were 405.45, 425.45, and 456.51, respectively and they are indicated in Table S1 for comparison with other models. Covariate screening analysis indicated that the age, gender, and liver function parameters did not affect on the PK parameters. NAT2 phenotypes and body weight were considered to be the significant influences on the apparent clearance (CL/F), and only body weight had a significant effect on the apparent volume of distribution (V_d/F). The final model with these covariate decreased the OFV, AIC and BIC by 63.84, 55.84, and 43.42, respectively. The number of parameter was increased from 10 to 14 after the base model was updated to be the final model. The detailed PopPK parameter estimates derived from the final model are given in Table 3.

3.2.1. Model validation

The GOF plots presented in Figure 1 revealed acceptable agreement between the predicted and observed concentrations. The CWRES were generally distributed around zero with no trend, and the majority of them were in the -2 to +2 range. The results of bootstrap analysis are expressed in Table 3. All parameter estimates obtained from the final PopPK model were within the 95% confidence intervals (CI) generated by the bootstrap analysis and were close to the median values, with minimal bias (<10%), indicating the robust stability of the final model. However, we concerned about Vd/F random effect shown 24.7% bias, suggesting instability in estimating between-subject variability for V_d/F. This likely reflects the sparse sampling design. The VPC plots were illustrested in Figure 2. All the observation values of INH and those stratified with NAT2 phenotypes were well distributed within 90% prediction intervals (of 5-95%) of prediction values.

3.3. Model-based simulation of INH dosage

The PopPK parameters in Table 2 derived from the final model by Phoenix® NLME were applied in the Oracle® Crystal Ball software to simulate proper INH dosage regimens. Monte Carlo simulations based on a one-compartment PK model were conducted to estimate optimal INH dosage regimens through the calculation of PK parameters and plasma C−T profiles. The PP3−6, PP6, PPA10, and %PTA50 were considerable simulated outcomes of the INH dosing simulation in each NAT2 phenotype. Dosage regimen simulations for oral administration were conducted at dosing intervals of every 8, 12, and 24 hours with various doses of INH for

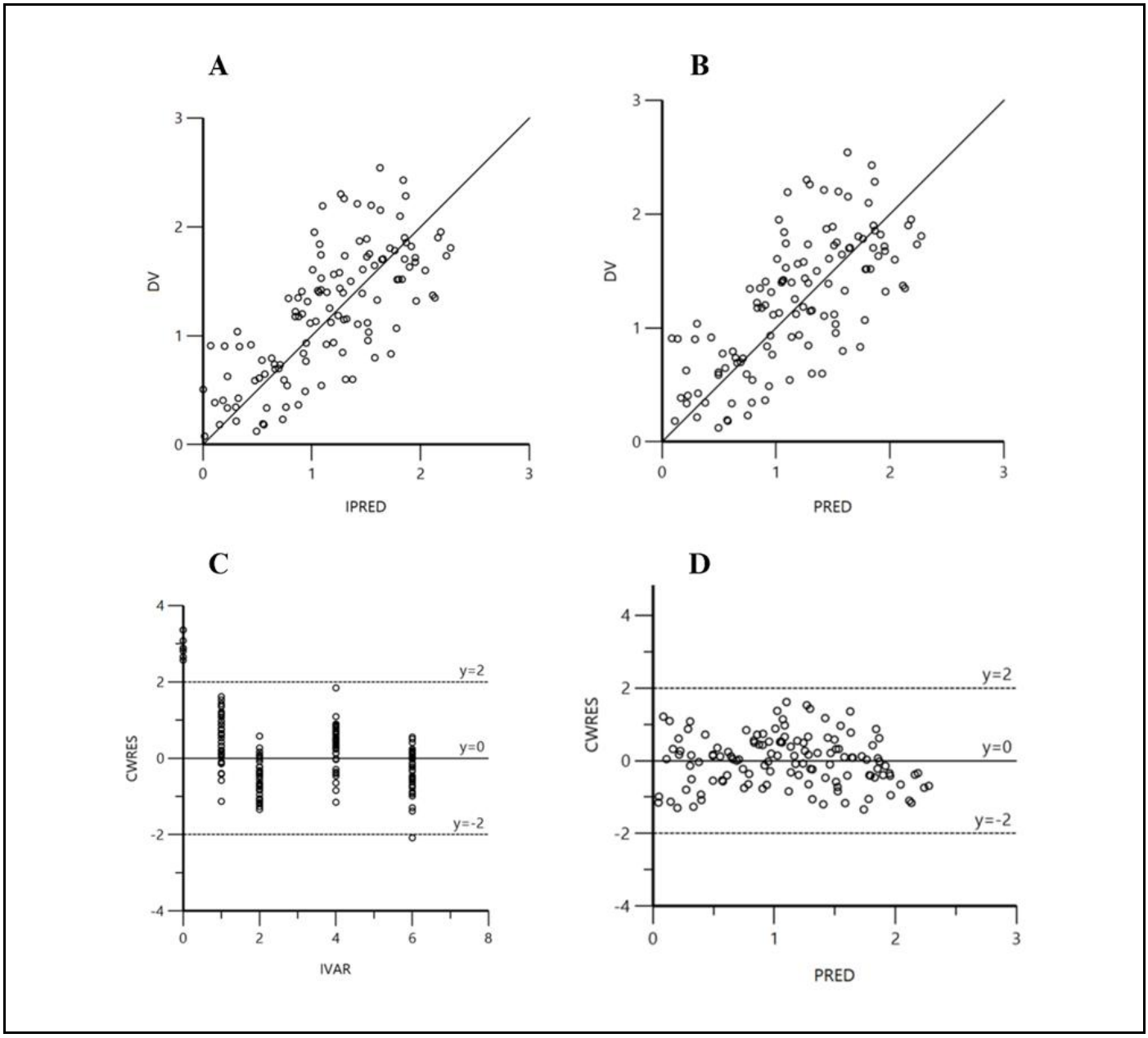

Figure 1. Goodness-of-fit plots of the final model for INH (A) Observed data (DV) versus Individual population predictions (IPRED) (B) DV versus Population predictions (PRED) (C) Conditional weighted residuals (CWRES) versus Time (IVAR) (D) CWRES versus PRED.

each NAT2 phenotype. However, the differences among these dosing intervals were not statistically significant. Therefore, subsequent INH dosing simulations with various doses were performed only at 24-hour intervals, as presented in Tables S2 and S3.

The appropriate dosage regimen was selected based on efficiency and safety outcomes. For efficacy, the PP3−6, PPA10, and %PTA50 presented the INH activity in which the more value indicated the better rate of successful treatment. The investigating points for the PP3−6, PPA10, and %PTA50 were in approximately or not less than 80% [11]. Data are presented in Figures 3−5. For safety, the PP6 represented the percentage of adverse drug reaction (ADR) occurrence in which the less value indicated the lower rate of ADR. The prevalence of drug induced liver injury (DILI) was reported in approximately of 36%, 19%, and 20% for SA, IA, and RA, respectively [18]. Therefore, the cutoff value for the PP6 was less than 19%.

The INH dosing simulations were performed using Oracle® Crystal Ball based on the pharmacokinetic parameters obtained from the final model. For the SA group, the efficacy indicators PP3–6, PPA10, and %PTA50 were 67.84%, 21.93%, and 100%, respectively, for an INH dosage regimen of 300 mg every 24 hours. However, within the dosage range of 225–250 mg, the PP3–6 values increased to 81.61–82.82%, while the PPA10 and %PTA50 values ranged from 2.60–6.49% and 100%, respectively. At INH doses exceeding 275 mg, the proportion of patients within the

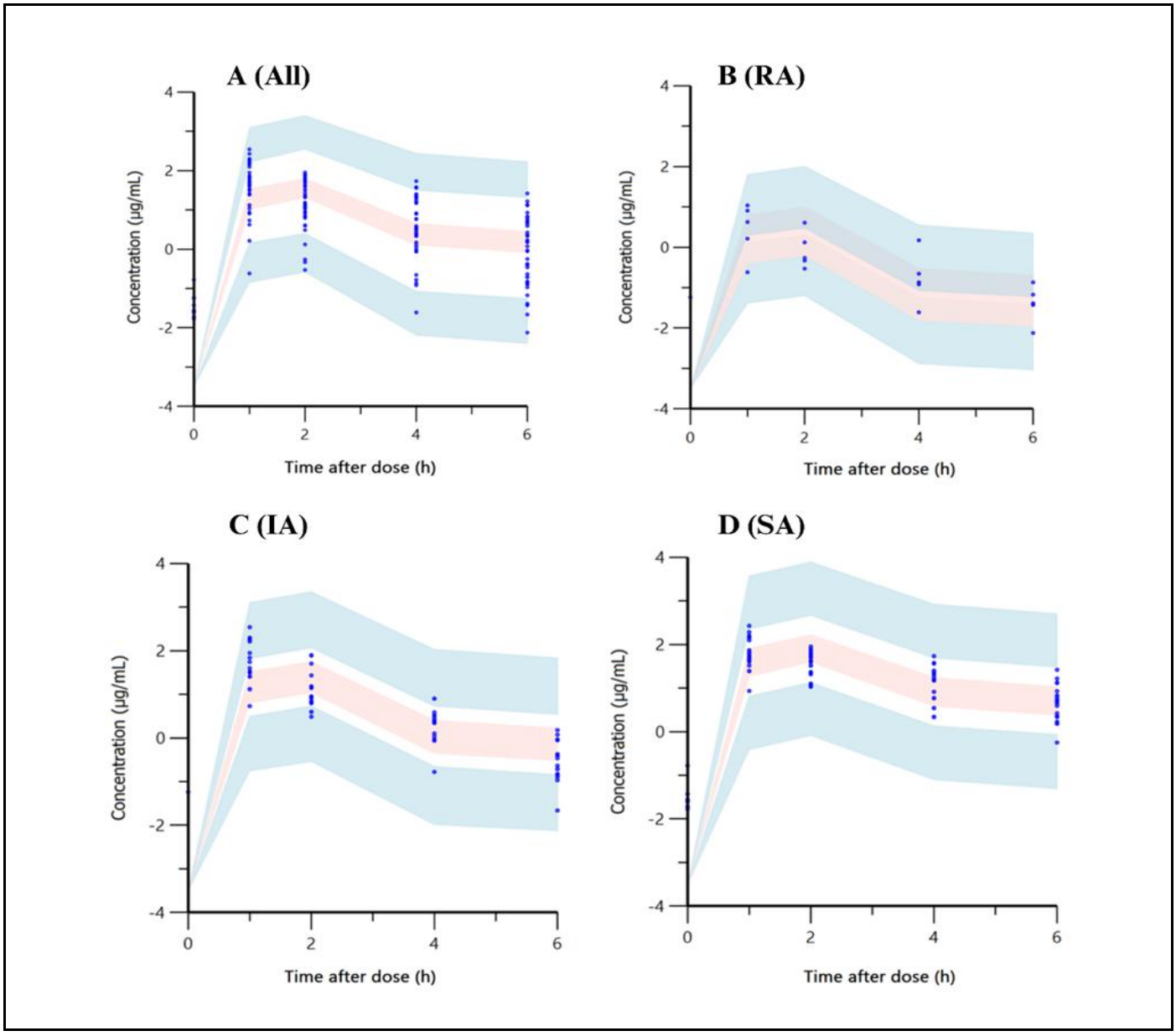

Figure 2. Visual predictive check (VPC) of (A) the final model and stratified VPC of (B) RA, (C) IA, and (D) SA. The dot on the graph represent observations. Blue shaded areas represent 95%CIs for the predicted 95th and 5th percentiles. Red shaded area represents 95%CI for the predicted 50th percentile.

PP3–6 range decreased due to INH concentrations surpassing 6 µg/mL. Regarding safety, the PP6 for the 225–250 mg INH regimens indicated an ADR risk of less than 12%, with the 225 mg regimen showing a risk below 5%. Therefore, the optimal INH dosage regimen for the SA group was determined to be 225–250 mg administered every 24 hours.

For the IA group, the efficacy parameters PP3–6, PPA10, and %PTA50 were 84.55%, 0.25%, and 99.99%, respectively, for an INH dosage regimen of 275 mg every 24 hours. Within the dosage range of 275–300 mg, the PP3–6 values ranged from 83.01% to 84.55%, the PPA10 from 0.25% to 0.67%, and the %PTA50 from 99.99% to 100%. At INH doses exceeding 300 mg, the proportion of patients within the PP3–6 range declined to below 80% due to INH concentrations surpassing 6 µg/mL, consistent with findings in the SA group. Regarding safety, the PP6 values for 275–300 mg INH ranged from 6.43% to 12.31%, remaining below the threshold associated with a significant risk of ADR. Higher doses resulted in PP6 values exceeding 20%. Therefore, the optimal INH dosage regimen for the IA group was determined to be 275–300 mg administered every 24 hours.

For the RA group, the efficacy parameters PP3–6 and %PTA50 were 90.72% and 100%, respectively, for an INH dosage regimen of 400 mg every 24 hours. Increasing the INH dose to 450 mg resulted in an 8.66% increase in the PP3–6 value compared with the 400 mg regimen. Regarding safety, PP6 values for both 400 mg

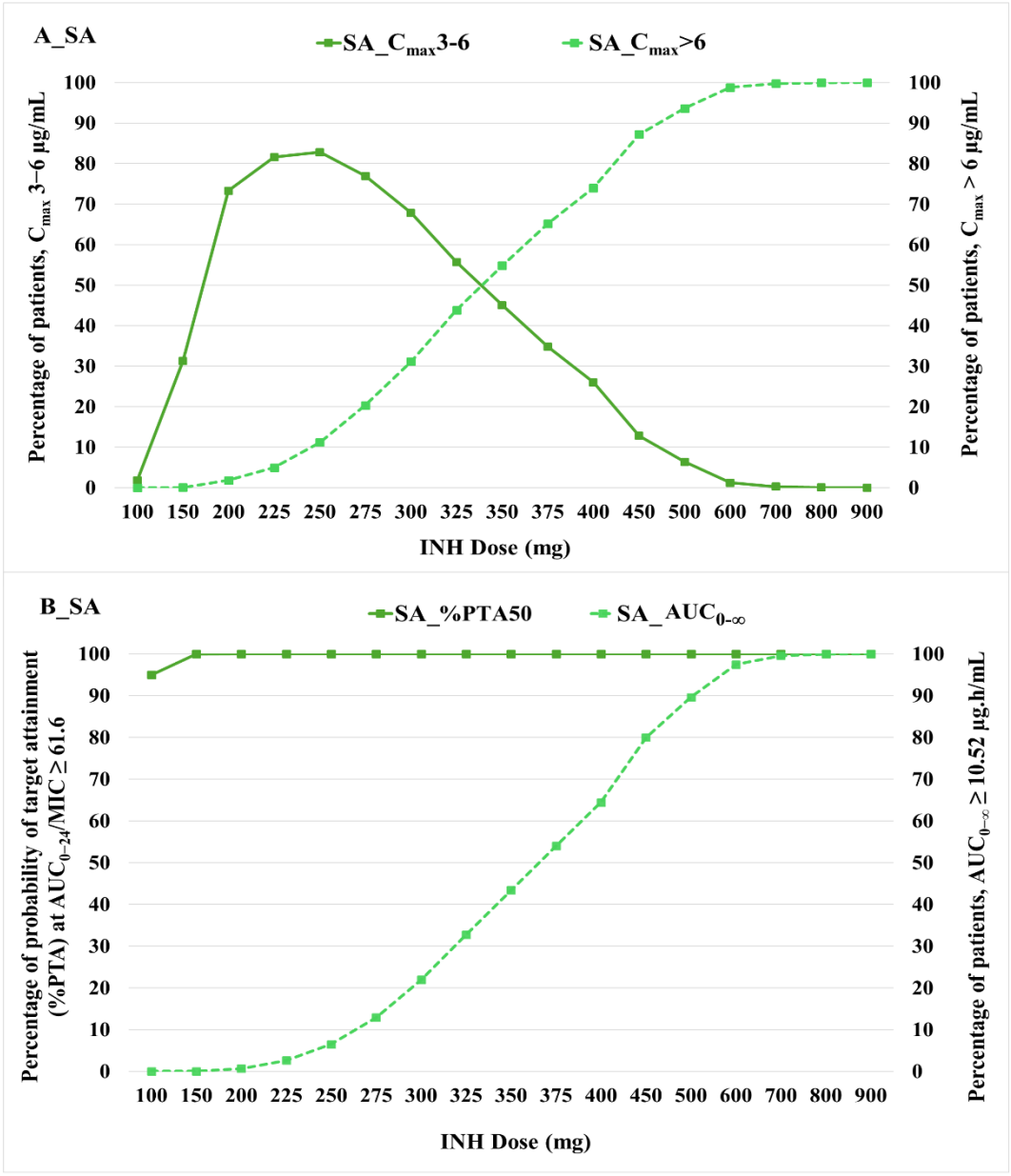

Figure 3. Isoniazid dosing simulation on the percentage of patients who achieved C_{max} between 3 and 6 µg/mL vs C_{max} > 6 µg/mL for SA (A) and $AUC_{0–24}$/MIC > 61.6 (%PTA50) vs $AUC_{0–\infty} \geq 10.52$ µg.h/mL for SA (B). Abbreviation: $AUC_{0–\infty}$: area under the curve from 0 to infinity hour, $AUC_{0–24}$: area under the curve from 0 to 24 hours, C_{max}: maximum plasma concentration; MIC: minimum inhibition concentration; PTA: probability of target attainment; SA: slow acetylator.

and 450 mg INH were undetectable, indicating no apparent risk of ADR. In terms of efficacy, the 400 mg regimen showed a slightly lower likelihood of achieving effective treatment outcomes compared with the 450 mg regimen. Therefore, the optimal INH dosage regimen for the RA group was considered to range from 400 to 450 mg administered every 24 hours.

4. DISCUSSION

The present study developed a PopPK model to characterize the PK of isoniazid in Thai pulmonary TB patients, employing a one-compartment structural model with first-order absorption and elimination with FOCE-ELS algorithm and log-additive residual error with incorporating the covariates of weight and NAT2 phenotype. The final model produced reductions in OFV, AIC, and BIC of 63.84, 55.84, and 43.42 units, respectively. The OFV reduction substantially exceeded the pre-specified significance threshold of 3.84 units (chi-squared distribution, $p < 0.05$, df = 1), providing strong statistical evidence that the inclusion of these covariates yielded a significantly superior model fit. Critically, the concurrent and substantial reductions in

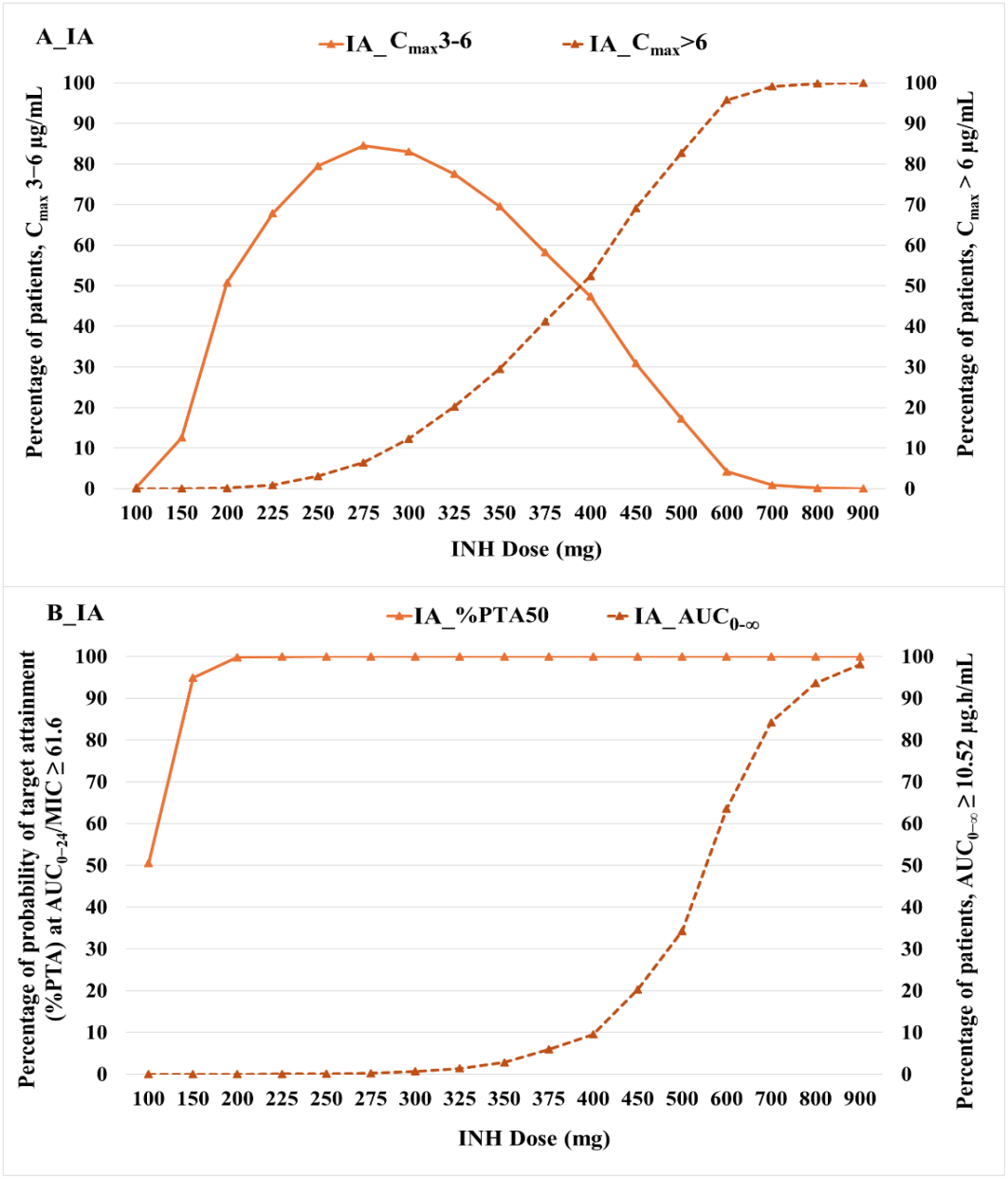

Figure 4. Isoniazid dosing simulation on the percentage of patients who achieved C_{max} between 3 and 6 µg/mL vs C_{max} > 6 µg/mL for IA (A) and $AUC_{0–24}$/MIC > 61.6 (%PTA50) vs $AUC_{0–\infty}$ ≥ 10.52 µg.h/mL for IA (B). Abbreviation: $AUC_{0–\infty}$: area under the curve from 0 to infinity hour, $AUC_{0–24}$: area under the curve from 0 to 24 hours, C_{max}: maximum plasma concentration; IA: intermediate acetylator; MIC: minimum inhibition concentration; PTA: probability of target attainment.

both AIC and BIC confirmed that this improvement in fit was not achieved at the cost of overparameterization. The convergence of all three information criteria in favor of the final model provided robust statistical support for the covariate structure adopted.

Isoniazid disposition was described using a two-compartment model with first-order absorption and elimination in most of the published PopPK studies [11, 19-23]; nonetheless, the adoption of a one-compartment structural model in the present analysis was scientifically justified and consistented with those studies conducted under analogous sparse sampling conditions. The identifiability of a two-compartment model critically depended on the availability of blood samples that captured the distribution phase necessary to identify a peripheral compartment, which for isoniazid occurred within approximately 15–30 minutes of oral administration [23]. In the present study, the earliest post-absorption sample was collected at 1 hour post-dose, by which point distribution equilibrium was largely complete. Under these sampling constraints, adding a peripheral compartment would introduce parameters

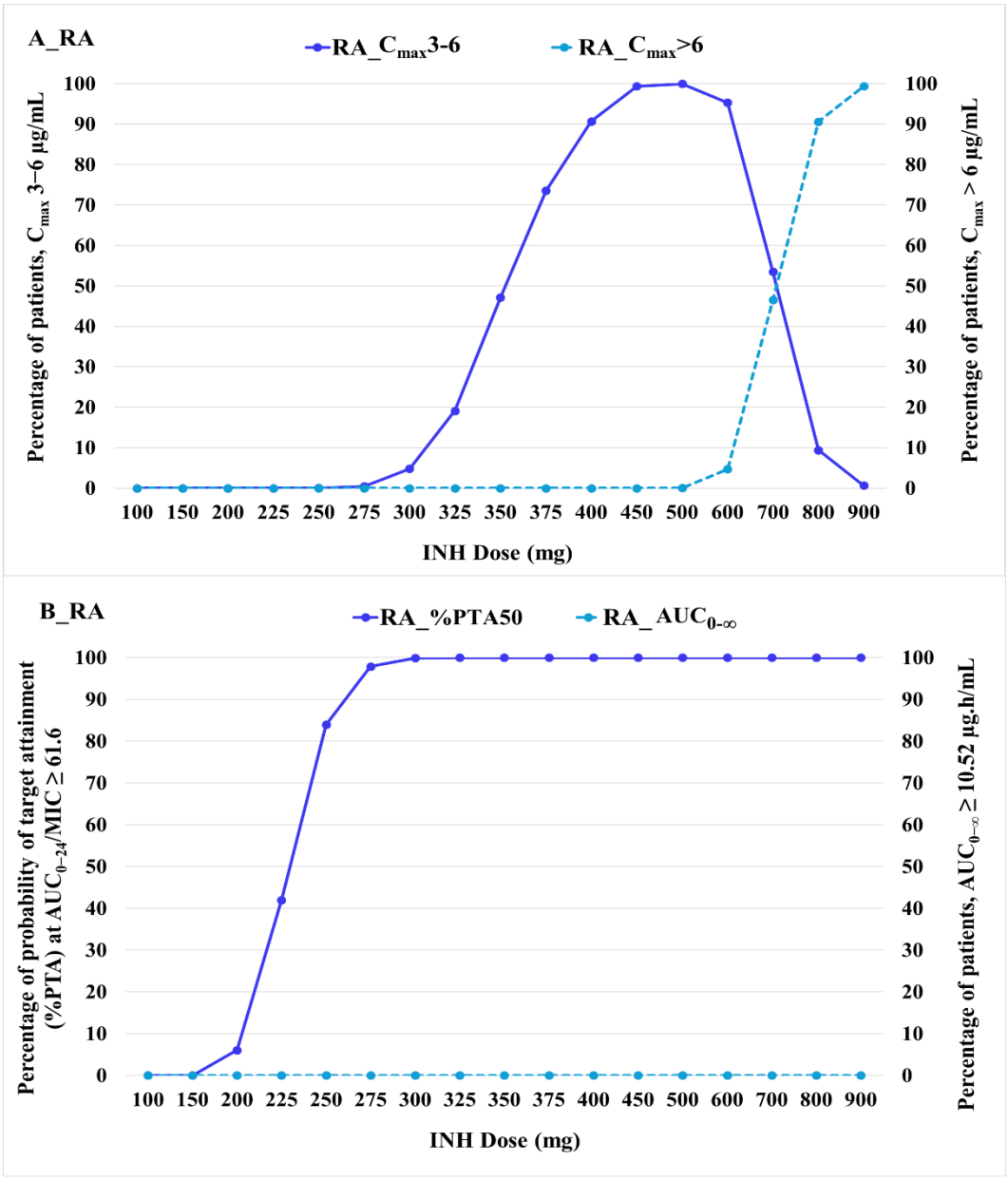

Figure 5. Isoniazid dosing simulation on the percentage of patients who achieved C_{max} between 3 and 6 µg/mL vs C_{max} > 6 µg/mL for RA (A) and $AUC_{0–24}$/MIC > 61.6 (%PTA50) vs $AUC_{0–\infty} \geq 10.52$ µg.h/mL for RA (B). Abbreviation: $AUC_{0–\infty}$: area under the curve from 0 to infinity hour, $AUC_{0–24}$: area under the curve from 0 to 24 hours, C_{max}: maximum plasma concentration; MIC: minimum inhibition concentration; PTA: probability of target attainment; RA: rapid acetylator.

that could not be reliably estimated from the available data, substantially increasing the risk of model overparameterization, numerical instability, and inflated parameter uncertainty. Model comparisons based on the OFV and population-level predictions represented the most appropriate evaluation tools under such conditions, and both strongly favored the one-compartment structure. The adequacy of this model was further confirmed empirically by satisfactory GOF diagnostics, low residual variability (CV% = 6.8%), and strong bootstrap parameter stability, providing convergent evidence that the one-compartment model was structurally sufficient for describing isoniazid pharmacokinetics under the study's sampling conditions. Moreover, our study showed the similar popPK model with one compartment as an Indonesian study [24], which was a study of sparse sampling design.

The estimated k_a was 1.586 h^{-1} (CV% = 6.1%), corresponding to an absorption half-life of approximately 26 minutes, indicating relatively rapid oral absorption of isoniazid consistent with its known physicochemical properties as a small, hydrophilic

molecule. The k_a ranging from 0.25 to 3.9 h^{-1} were reported in INH popPK studies [11, 19-21, 24, 25]. The V_d/F was 17.384 L (CV% = 6.7%), suggesting a predominantly central distribution pattern with limited peripheral tissue acclumulation at the population level, a value reflecting the lower median body weight of the Thai study population (median 53.09 kg). While, Indonesian study reported V_d/F of 40.5 L using a one-compartment structure [24].

Internal model validation by bootstrap resampling (n = 1,000) demonstrated strong parameter stability for all fixed-effect estimates. Bootstrap medians closely reproduced the final model point estimates, and parameter biases were consistently below 3% for all structural and covariate fixed effects, confirming that the OFV reductions and parameter estimates reflected robust pharmacokinetic signal in the Thai TB population. Two specific bootstrap findings should be concerned. First, the wide 95% confidence interval for k_a (1.335–24.607 h^{-1}) reflects genuine imprecision in absorption rate estimation arising from the absence of sampling points within the first 60 minutes post-dose, a constraint inherent to the clinical sampling design. Second, the random-effect estimate for V_d/F exhibited a bootstrap bias of 24.7%, with its 95% confidence interval crossing zero, indicating that between-subject variability in V_d/F could not be reliably characterized under the present sparse sampling design. However, both observations were consistent with known constraints of fixed-interval sparse sampling and did not undermine the validity of the fixed-effect covariate estimates, which were robustly and reproducibly determined. The GOF plots additionally provided indirect empirical support for the one-compartment structural model. If a two-compartment structure had been pharmacokinetically necessary, a systematic misfit would be expected, specifically with underprediction at 1 hour followed by overprediction at 2 hours, reflecting an inability to capture distribution-phase kinetics. The absence of this pattern in both the DV–PRED and CWRES–IVAR plots further supported the structural adequacy of the one-compartment model under the present sampling conditions.

Among all covariates examined, NAT2 acetylator phenotype emerged as the most statistically dominant and clinically consequential determinant of INH clearance. The OFV reduction upon NAT2 inclusion far exceeded that of any other covariate, consistent with the global consensus that the variability in INH disposition could be majorly attributed to NAT2 genotype, producing a trimodal clearance pattern with a multi-fold increase in clearance of RA compared to SA [22]. At the median body weight of 53.09 kg, predicted CL/F was 106.034 L/h for RA, 54.6 L/h for IA, and 30.7 L/h for SA patients, representing a 3.45-fold difference between RA and SA phenotypes. This was directly consistent with the twofold to threefold range reported in the global literature and fell within the pharmacokinetically expected range for this enzyme polymorphism [22].

The phenotype-specific clearance values estimated in the present Thai cohort could be meaningfully compared with those reported in published PopPK studies from other ethnic groups, and such comparison revealed a picture of both remarkable consistency in the direction and relative magnitude of NAT2 effects, and quantitatively important differences in absolute clearance values that had direct practical dosing implications.

Compared with a Chinese pulmonary tuberculosis cohort [26], the estimated CL/F of isoniazid was 18.2 L/h and the V_2/F was 56.8 L in a two-compartment model, both of which were substantially lower than the estimates observed in the present Thai cohort. However, direct numerical comparison was limited by two key methodological differences. First, the Chinese study used a two-compartment model in which clearence represented elimination from the central compartment only, whereas in a one-compartment model clearence reflected total apparent clearance and incorporated distributional effects. Second, the Chinese population had a different body weight distribution, and clearance was not stratified by NAT2 phenotype using the same parameterization as in the present analysis. Despite these differences, the relative impact of NAT2 within the Chinese cohort, where genotype produced the largest reduction in OFV among all covariates, was consistent with the strong pharmacogenetic effect observed here. This agreement supported a similar qualitative pharmacogenetic pattern across Asian populations, even though absolute clearance estimates varied according to model structure.

In PopPK analysis of South Africa population, Abdelwahab et al. [27] reported isoniazid CL/F of 97.1 L/h, 75.7 L/h, and 29.0 L/h for RA, IA, and SA, respectively. When compared with the corresponding estimates from the present Thai cohort, a clear pattern emerged. CL/F estimates for RA and SA were broadly consistent across the two populations, with a modestly higher value for RA in the Thai cohort (106.0 vs. 97.1 L/h) and nearly identical values for SA (30.7 vs. 29.0 L/h). In contrast, the CL/F for IA in the Thai cohort (54.6 L/h) was substantially lower than the 75.7 L/h reported by Abdelwahab and colleagues. The difference likely reflected underlying population-level variation in the genetic composition of the IA group. This phenotype was inherently heterogeneous, comprising multiple heterozygous NAT2 haplotype combinations with varying residual enzymatic activity. Differences in the distribution of these haplotypes between Thai and other populations may have explained the observed divergence in clearance within this subgroup.

The most geographically and ethnically relevant comparator for Thai patients was the Indonesian cohort reported by Soedarsono and colleagues [24]. This population shared similar body weight (median ~50 kg), high tuberculosis burden, and comparable *NAT2* genotype distribution characteristic of Southeast Asia. In that study, isoniazid CL/F for RA, IA, and SA was 55.9, 37.8, and 17.7 L/h, respectively, using a one-compartment model with allometric scaling, with NAT2 significantly influencing clearance. In comparison, the Thai cohort showed consistently higher CL/F, corresponding to ~1.9-, 1.4-, and 1.7-fold increases for RA, IA, and SA. Despite these differences, the relative pharmacogenetic pattern was preserved. The rapid-to-intermediate ratio was larger in Thailand (1.9 vs. 1.5), whereas the rapid-to-slow ratio was similar (3.45 vs. 3.2), aligning with global estimates. This consistency indicated that the pharmacogenetic influence of NAT2 on INH elimination remained structurally stable across Southeast Asian populations. Higher Thai clearance likely reflected methodological and biological factors, including different allometric scaling approaches, and inter-population differences in NAT2 allele composition. Sub-ethnic variability further contributed to heterogeneity, limiting cross-population extrapolation.

The Indian popPK study by Thomas et al. [23] offers a valuable comparison, given similarities with Thailand in tuberculosis burden, genetic diversity, and representation of *NAT2* genotype groups. In that study, isoniazid PK were described using a two-compartment model with transit absorption, yielding CL/F estimates of 36.3, 23.2, and 16.5 L/h for RA, IA, and SA. These values were markedly lower than those observed in the Thai cohort. Although the rapid-to-slow clearance ratio was smaller in India (2.2-fold vs. 3.45-fold in Thailand), direct comparison was limited by structural model differences, as two-compartment clearance reflected central elimination only, whereas one-compartment clearance represented total apparent clearance. Although *NAT2* genotype was evaluated in the Indian model, it did not meet statistical inclusion criteria, likely due to limited sample size and sparse sampling rather than absence of a true effect. This contrasts with the Thai study, where *NAT2* showed a strong and statistically significant influence. Phenotype distribution also differed between populations. IA predominated in India, whereas SA were more common in Thailand. This higher proportion of SA in the Thai cohort may have increased the population-level risk of supratherapeutic exposure and hepatotoxicity under standard dosing.

Taken together, cross-ethnic comparisons showed a consistent global pattern: *NAT2* genotype was the primary determinant of isoniazid clearance, producing a trimodal distribution across all populations. The relative effect size was stable, with RA showing approximately 1.5 to 2-fold higher clearance than IA and 2 to 3.5-fold higher than SA. However, absolute clearance values varied across populations due to differences in body composition, underlying genetic architecture within phenotype groups, clinical context, and model structure. As a result, model-informed dosing strategies needed to rely on population-specific pharmacokinetic models rather than extrapolation from other ethnic groups. The present study addresseed this gap for Thailand and establishes a foundation for precision dosing in Thai TB patients.

Some limitations of the present analysis had to be acknowledged. First, the total sample size of 39 patients, while sufficient to support PopPK estimation and detect the dominant NAT2 and body weight covariate effects, was relatively small for robust covariate modeling, particularly given the unequal distribution across NAT2 phenotype groups and the highly restricted representation of rapid acetylators (n = 5). Future studies should target sample sizes of at least 60–80 patients with balanced phenotype group enrollment to improve covariate stability and support exploration of potential pharmacokinetic interactions. Second, the sparse sampling window of 0–6 hours was insufficient to characterize the absorption phase with precision, as evidenced by the wide bootstrap CI for k_a and did not extend beyond one INH elimination half-life in the RA, potentially introducing minor estimation bias in structural parameters. Future study designs should have incorporated at least one early sample within the first 30 minutes post-dose to improve absorption characterization and extended sampling window to a minimum of 8 hours to cover the true INH elimination half-life in the RA. In addition, the last sampling point should have exeeeded 15 hours to obtain a reliable characterization of the elimination phase, particularly in the SA, where the half-life was approximately 2-5 hours [24, 28, 29]. Finally, the high bootstrap bias for the V_d/F random effect (24.7%) suggested instability in estimating Vd/F variability, potentially due to limited sampling during the distribution phase. Further model refinement is needed.

To thoroughly determine the dosage regimen of INH that affected by NAT2 phenotype on CL/F, the popPK estimations for each phenotypes were simulated separately. The INH dosing simulation using Oracle® Crystal Ball, based on the PK parameters from the final model. The simulated results for the regular INH dose of 300 mg/day showed suboptimal outcomes in the RA group and enhance toxicity in the SA group. The criticized data from our dosing simulations across various regimens for specific NAT2 acetylator groups suggested that INH dosage regimens should be adjusted to optimize the rate and extent of INH absorption into systemic circulation, enabling personalized treatment

for Thai TB patients. In recent guidelines, the standard dose of INH in patients with TB was 4−6 mg/kg/day or 300 mg/day [2, 3]. Our analysis of the IA group revealed that the efficacy outcomes, represented by PP3-6, PPA10, and %PTA50, along with the safety concern indicated by PP6, suggested that the optimal TB treatment dosage regimen was 275-300 mg of INH every 24 hours. Therefore, the INH dosage regimen of 275-300 mg every 24 hours for the IA group was in accordance with the guideline. However, a slight reduction of standard dose may have been appropriate due to findings that the activity of the NAT2 enzyme varied depending on the genotype, forming a gradient of enzymatic efficiency. *NAT2* genotypes such as NAT2*6A and NAT2*7B were classified as ultraslow haplotypes, while NAT2*5B was categorized as a slow haplotype. The enzymatic activity of NAT2 variants in metabolizing INH ranged from least to most effective as follows: NAT2*7 < NAT2*6 < NAT2*5 < NAT2*4. When a slow-activity allele paired with the wild-type NAT2*4, overall enzyme activity could have been reduced, resulting in an IA phenotype [7, 30]. In Europe populations, NAT2*5 was the most prevalent variant, supporting the use of a lower INH dose to reduce drug-induced liver injury (DILI) risk. In contrast, NAT2*6 and NAT2*7 were more common in the Thai population [6, 9, 30, 31], indicating that the INH dose of 275-300 mg/day may have been more appropriate in this setting. Moreover, a study on the Korean population PK also suggested that 300 mg/day of INH was an appropriate dosage regimen for IA individuals in the treatment of drug-susceptible tuberculosis [11]. On the other hand, the SA and RA groups required regimen adjustments, as the simulation results with a dosage of 300 mg INH every 24 hours indicated subtherapeutic and supratherapeutic INH concentrations in the RA and SA groups, respectively. For the SA group, a reduction of the INH dose from 300 mg to 250 mg was recommended. Several studies reported that reducing the INH dose in the SA group could decrease the incidence of hepatotoxicity while ensuring the C_{max} of INH remained below 6 μg/mL [10, 15]. Azuma J and colleagues administered INH 2.5 mg/kg/day (50% dose reduction from the standard INH dose of 5 mg/kg/day) in the SA group and found that this group did not show DILI, compared with the SA group receiving the standard INH dose, which presented the DILI incidence of 77.80% [15]. In addition, Cho YS and colleagues conducted a Korean population PK modeling study and suggested that the optimal INH dosage regimen in SA group was 200 mg every 24 hours [11]. This dose adjustment may have decreased the risk of INH-induced toxicity, reflected by an approximate 20% reduction in PP6, while preserving therapeutic efficacy at a level comparable to that achieved with the standard dose proposed for the IA group. For the RA group, the efficacy and the safety indicators suggested that the optimal TB treatment dosage was 400-450 mg INH every 24 hours. Some studies reported subtherapeutic concentrations with the standard 300 mg INH dosing in the RA group, leading to an increased the risk of treatment failure and the development of INH resistance [10, 32, 33]. Azuma J and colleagues suggested INH 7.5 mg/kg/day which was equivalent to 450 mg in patients weighing 60 kg [15]. Moreover, Cho YS and colleagues recommended a simulated INH dose of 400 mg once daily in RA patients with TB for Korean population [11]. Therefore, increasing the INH dose to 400-450 mg/day could help elevate INH plasma concentrations into the therapeutic range, improving treatment success rates and reducing the likelihood of resistance. Moreover, this dosage adjustment may help mitigate the association observed between NAT2 rapid acetylator status and retreatment or treatment failure, accentuating the role of inadequate drug exposure in fixed-dose regimens [34].

5. CONCLUSION

The final one-compartment popPK model for INH in Thai pulmonary TB patients was robust, clinically interpretable, and well validated. Model adequacy was supported by consistent reductions in OFV, AIC, and BIC with covariate inclusion, satisfactory GOF diagnostics, low residual variability, and stable bootstrap estimates, confirming reliability despite sparse sampling. NAT2 phenotype and body weight were the principal determinants of PK variability, with a 3.45-fold difference in CL/F between RA and SA, spotlighting the need for dose individualization and hepatotoxicity risk management. The observed pharmacogenetic pattern, with a predominance of SA, aligned with other Asian and African populations, supporting the global consistency of NAT2 effects while emphasizing population-specific phenotype distributions. Monte Carlo simulations based on the final model suggested optimal dosing of 275–300 mg once daily for IA, 225–250 mg for SA, and 400–450 mg for RA. These findings provided a quantitative basis for NAT2-guided, weight-adjusted isoniazid dosing in Thailand and supported further prospective studies to refine precision dosing strategies and to pave the way for integrating pharmacogenetics into clinical practice for guiding INH dosing in TB treatment.

6. ACKNOWLEDGEMENTS

The author gratefully acknowledges the equipment support from the Pharmacometrics Center, faculty of pharmacy, Mahidol University and the BioRender licensed by the faculty of medicine, Thammasat University to create the graphic abstract.

Author contribution
T.S., P.T., and W.N. designed the research and wrote the manuscript. T.S., and W.N. performed the research, analyzed and discussed the data. P.T., and W.N. approved the manuscript. S.M., H.S., and U.U. contributed patient data.

Funding
No funding was received for this work.

Conflict of interest
The authors declared no competing interests for this work.

Ethics approval
The study was conducted under the IRB ethical approval (COE.NO.MU-DT-PY-IRB 2023/043.0410).

Article info:
Received December 31, 2025
Received in revised form April 27, 2026
Accepted April 6, 2026

REFERENCES

1. Kalscheuer R, Palacios A, Anso I, Cifuente J, Anguita J, Jacobs WR, et al. The *Mycobacterium tuberculosis* capsule: a cell structure with key implications in pathogenesis. Biochem J. 2019;476(14):1995-2016.
2. Division of Tuberculosis. National tuberculosis control programme guideline, Thailand 2021. Bangkok: Division of tuberculosis; 2021.
3. WHO consolidated guidelines on tuberculosis: Module 4: Treatment - drug-susceptible tuberculosis treatment. WHO guidelines approved by the guidelines review committee. Geneva, 2022.
4. Erwin ER, Addison AP, John SF, Olaleye OA, Rosell RC. Pharmacokinetics of isoniazid: The good, the bad, and the alternatives. Tuberculosis (Edinb). 2019;116S:S66-S70.
5. Gutierrez-Virgen JE, Pina-Pozas M, Hernandez-Tobias EA, Taja-Chayeb L, Lopez-Gonzalez ML, Meraz-Rios MA, et al. NAT2 global landscape: Genetic diversity and acetylation statuses from a systematic review. PLoS One. 2023;18(4):e0283726.
6. Wattanapokayakit S, Mushiroda T, Yanai H, Wichukchinda N, Chuchottawon C, Nedsuwan S, et al. NAT2 slow acetylator associated with anti-tuberculosis drug-induced liver injury in Thai patients. Int J Tuberc Lung Dis. 2016;20(10):1364-9.
7. Suvichapanich S, Wattanapokayakit S, Mushiroda T, Yanai H, Chuchottawon C, Kantima T, et al. Genomewide association study confirming the association of nat2 with susceptibility to antituberculosis drug-induced liver injury in Thai patients. Antimicrob Agents Chemother. 2019;63(8):e02692-18.
8. Ungcharoen U, Sriplung H, Mahasirimongkol S, Chusri S, Wichukchinda N, Mokmued P, et al. The influence of NAT2 genotypes on isoniazid plasma concentration of pulmonary tuberculosis patients in Southern Thailand. Tuberc Respir Dis. 2020;83:S55-S62.
9. Sanchat T, Chuchottaworn C, Mahasirimongkol S, Wattanapokayakit S. NAT2 genotype-guided INH dosage to reduce drug-induced liver injury in Thai patients. Sys Rev Pharm. 2021;12(9):523-7.
10. Jung JA, Kim TE, Lee H, Jeong BH, Park HY, Jeon K, et al. A proposal for an individualized pharmacogenetic-guided isoniazid dosage regimen for patients with tuberculosis. Drug Des Devel Ther. 2015;9:5433-8.
11. Cho YS, Jang TW, Kim HJ, Oh JY, Lee HK, Park HK, et al. Isoniazid population pharmacokinetics and dose recommendation for Korean patients with tuberculosis based on target attainment analysis. J Clin Pharmacol. 2021;61(12):1567-78.
12. Ohno M, Yamaguchi J, Yamamoto I, Fukuda T, Yokota S, Maekura R, et al. Slow N-acetyltransferase 2 genotype affects the incidence of isoniazid and rifampicin-induced hepatotoxicity. Int J Tuberc Lung Dis. 2000;4(3):256-61.
13. Higuchi N, Tahara N, Yanagihara K, Fukushima K, Suyama N, Inoue Y, et al. NAT2*6A, a haplotype of the N-acetyltransferase 2 gene, is an important biomarker for risk of anti-tuberculosis drug-induced hepatotoxicity in Japanese patients with tuberculosis. World J Gastroenterol. 2007;13(45):6003-8.
14. Sotsuka T, Sasaki Y, Hirai S, Yamagishi F, Ueno K. Association of isoniazid-metabolizing enzyme genotypes and isoniazid-induced hepatotoxicity in tuberculosis patients. In Vivo. 2011;25(5):803-12.
15. Azuma J, Ohno M, Kubota R, Yokota S, Nagai T, Tsuyuguchi K, et al. NAT2 genotype guided regimen reduces isoniazid-induced liver injury and early treatment failure in the 6-month four-drug standard treatment of tuberculosis: A randomized controlled trial for pharmacogenetics-based therapy. Eur J Clin Pharmacol. 2013;69(5):1091-101.
16. Wichukchinda N, Pakdee J, Kunhapan P, Imunchot W, Toyo-Oka L, Tokunaga K, et al. Haplotype-specific PCR for NAT2 diplotyping. Hum Genome Var. 2020;7:13.
17. Gumbo T. New susceptibility breakpoints for first-line antituberculosis drugs based on antimicrobial pharmacokinetic/pharmacodynamic science and population pharmacokinetic variability. Antimicrob Agents Chemother. 2010;54(4):1484-91.
18. Surarak T, Chumnumwat S, Nosoongnoen W, Tragulpiankit P. Efficacy, safety, and pharmacokinetics of isoniazid affected by NAT2 polymorphisms in patients with tuberculosis: A systematic review. Clin Transl Sci. 2024;17(4):e13795.
19. Huerta-Garcia AP, Medellin-Garibay SE, Ortiz-Alvarez A, Magana-Aquino M, Rodriguez-Pinal CJ, Portales-Perez DP, et al. Population pharmacokinetics of isoniazid and dose recommendations in Mexican patients with tuberculosis. Int J Clin Pharm. 2020;42(4):1217-26.
20. Jing W, Zong Z, Tang B, Wang J, Zhang T, Wen S, et al. Population pharmacokinetic analysis of isoniazid among pulmonary tuberculosis patients from China. Antimicrob Agents Chemother. 2020;64(3):e01736-19.
21. Gao Y, Davies Forsman L, Ren W, Zheng X, Bao Z, Hu Y, et al. Drug exposure of first-line anti-tuberculosis drugs in China: A prospective pharmacological cohort study. Br J Clin Pharmacol. 2021;87(3):1347-58.
22. Thomas L, Raju AP, Chaithra, M SS, Varma M, Saravu K, et al. Influence of N-acetyltransferase 2 (NAT2) genotype/single nucleotide polymorphisms on clearance of isoniazid in tuberculosis patients: A systematic review of population pharmacokinetic models. Eur J Clin Pharmacol. 2022;78(10):1535-53.
23. Thomas L, Batcha JSD, Chaithra, Upadhyay S, Parate SS, Prasad TSK, et al. Population pharmacokinetics of isoniazid in adult Indian tuberculosis patients: Evaluation of NAT2 polymorphisms. Infect Genet Evol. 2026;138:105883.
24. Soedarsono S, Jayanti RP, Mertaniasih NM, Kusmiati T, Permatasari A, Indrawanto DW, et al. Development of population pharmacokinetics model of isoniazid in Indonesian patients with tuberculosis. Int J Infect Dis. 2022;117:8-14.

25. Naidoo A, Chirehwa M, Ramsuran V, McIlleron H, Naidoo K, Yende-Zuma N, et al. Effects of genetic variability on rifampicin and isoniazid pharmacokinetics in South African patients with recurrent tuberculosis. Pharmacogenomics. 2019;20(4):224-40.
26. Chen B, Shi HQ, Feng MR, Wang XH, Cao XM, Cai WM. Population pharmacokinetics and pharmacodynamics of isoniazid and its metabolite acetylisoniazid in Chinese population. Front Pharmacol. 2022;13:932686.
27. Abdelwahab MT, Leisegang R, Dooley KE, Mathad JS, Wiesner L, McIlleron H, et al. Population pharmacokinetics of isoniazid, pyrazinamide, and ethambutol in pregnant South African women with tuberculosis and HIV. Antimicrob Agents Chemother. 2020;64(3):e01978-19.
28. Kiser JJ, Zhu R, D'Argenio DZ, Cotton MF, Bobat R, McSherry GD, et al. Isoniazid pharmacokinetics, pharmacodynamics, and dosing in South African infants. Ther Drug Monit. 2012;34(4):446-51.
29. Alshaikheid M, Ben Fredj N, Hannachi I, Kolsi N, Ben Fadhel N, Kerkeni E, et al. Development of a population pharmacokinetic model and Bayesian estimators for isoniazid in Tunisian tuberculosis patients. Pharmacogenomics J. 2021;21(4):467-75.
30. Fukunaga K, Kato K, Okusaka T, Saito T, Ikeda M, Yoshida T, et al. Functional characterization of the effects of N-acetyltransferase 2 Alleles on N-acetylation of eight drugs and worldwide distribution of substrate-specific diversity. Front Genet. 2021;12:652704.
31. Nicoletti P, Devarbhavi H, Goel A, Venkatesan R, Eapen CE, Grove JI, et al. Genetic risk factors in drug-induced liver injury due to isoniazid-containing antituberculosis drug regimens. Clin Pharmacol Ther. 2021;109(4):1125-35.
32. Kinzig-Schippers M, Tomalik-Scharte D, Jetter A, Scheidel B, Jakob V, Rodamer M, et al. Should we use N-acetyltransferase type 2 genotyping to personalize isoniazid doses? Antimicrob Agents Chemother. 2005;49(5):1733-8.
33. Unissa AN, Sukumar S, Hanna LE. The Role of N-Acetyl transferases on isoniazid resistance from ycobacterium tuberculosis and human: An *in silico* approach. Tuberc Respir Dis (Seoul). 2017;80(3):255-64.
34. Wattanapokayakit S, Sawaengdee W, Kunhapan P, Prakongsup P, Kasamatsu A, Imsanguan W, et al. NAT2 rapid acetylator phenotype and increased risk of tuberculosis retreatment: A TB cohort study in Northern Thailand. Int J Infect Dis. 2025;161:108123.